

Direct extraction of transversity and its accompanying T-odd distribution from the unpolarized and single-polarized Drell-Yan processes

A. N. Sissakian,^{*} O. Yu. Shevchenko,[†] A. P. Nagaytsev,[‡] and O. N. Ivanov[§]

Joint Institute for Nuclear Research, 141980 Dubna, Russia

(Received 25 May 2005; revised manuscript received 22 August 2005; published 30 September 2005)

The Drell-Yan processes with unpolarized colliding hadrons and with the single transversally polarized hadron are considered. The possibility of direct (without any model assumptions) extraction of both transversity and its accompanying T-odd parton distribution functions is discussed. For Drell-Yan processes measurements planned at GSI, the preliminary estimations demonstrate that it is quite real to extract both transversity and its accompanying T-odd PDF in the PAX conditions.

DOI: [10.1103/PhysRevD.72.054027](https://doi.org/10.1103/PhysRevD.72.054027)

PACS numbers: 13.85.Qk, 13.60.Hb, 13.88.+e

The advantage of the Drell-Yan (DY) process for extraction of parton distribution functions (PDFs), is that there is no need for any fragmentation functions. While the double transversely polarized DY process $H_1^\dagger H_2^\dagger \rightarrow l^+ l^- X$ allows us to directly extract the transversity distributions (see Ref. [1] for review), in the single-polarized DY $H_1 H_2^\dagger \rightarrow l^+ l^- X$ the access to transversity is rather difficult since it enters the respective cross-section in the complex convolution with another unknown T-odd PDF (see below). At the same time it is certainly very desirable to manage to get the transversity PDF from unpolarized and single-polarized DY processes as an alternative possibility. Besides, T-odd PDFs are very intriguing and interesting objects in themselves, so it is also very important to extract them.

The main goal of this paper is to investigate the possibility to completely disentangle PDFs corresponding to the unpolarized and single-polarized DY processes.

Let us first consider the results of Ref. [2] for both unpolarized and single-polarized DY processes. In that paper the Collins-Soper frame¹ is used (see Fig. 3 in Ref. [2]), where one deals with three angles θ , ϕ , and ϕ_{S_2} . Two angles, θ and ϕ , are common for both unpolarized and polarized DY processes. These are the polar and azimuthal angles of the lepton pair. The third angle ϕ_{S_2} appears when hadron two is transversely polarized, and this is just the azimuthal angle of \mathbf{S}_{2T} measured with respect to the lepton plane.

We consider here the case of pure transverse polarization of hadron two, so that we put $\lambda_1 = 0$ and $|\mathbf{S}_{1T}| = 1$ ($\lambda_2 = 0$ and $|\mathbf{S}_{2T}| = 1$ in our notation) in the respective equations of Ref. [2] (Eqs. (21) and (22) in Ref. [2]) for unpolarized and single-polarized cross-sections. Besides, taking into account only the dominating electromagnetic contributions and neglecting (just as in Ref. [2]) the ‘‘higher harmonic’’

term containing 3ϕ -dependence, one gets the following simplified equations for the QPM unpolarized and single-polarized cross-sections

$$\begin{aligned} \frac{d\sigma^{(0)}(H_1 H_2 \rightarrow l\bar{l}X)}{d\Omega dx_1 dx_2 d^2\mathbf{q}_T} &= \frac{\alpha^2}{12Q^2} \sum_q e_q^2 \left\{ (1 + \cos^2\theta) \right. \\ &\times \mathcal{F}[\bar{f}_{1q} f_{1q}] + \sin^2\theta \cos(2\phi) \\ &\times \mathcal{F}\left[(2\hat{\mathbf{h}} \cdot \mathbf{k}_{1T} \hat{\mathbf{h}} \cdot \mathbf{k}_{2T} \right. \\ &\left. \left. - \mathbf{k}_{1T} \cdot \mathbf{k}_{2T} \right) \frac{\bar{h}_{1q}^\perp h_{1q}^\perp}{M_1 M_2} \right] \left. \right\}, \quad (1) \end{aligned}$$

and

$$\begin{aligned} \frac{d\sigma^{(1)}(H_1 H_2^\dagger \rightarrow l\bar{l}X)}{d\Omega d\phi_{S_2} dx_1 dx_2 d^2\mathbf{q}_T} &= \frac{\alpha^2}{12Q^2} \sum_q e_q^2 \left\{ (1 + \cos^2\theta) \mathcal{F}[\bar{f}_{1q} f_{1q}] \right. \\ &+ \sin^2\theta \cos(2\phi) \mathcal{F}\left[(2\hat{\mathbf{h}} \cdot \mathbf{k}_{1T} \hat{\mathbf{h}} \cdot \mathbf{k}_{2T} \right. \\ &\left. \left. - \mathbf{k}_{1T} \cdot \mathbf{k}_{2T} \right) \frac{\bar{h}_{1q}^\perp h_{1q}^\perp}{M_1 M_2} \right] + (1 + \cos^2\theta) \\ &\times \sin(\phi - \phi_{S_2}) \mathcal{F}\left[\hat{\mathbf{h}} \cdot \mathbf{k}_{2T} \frac{\bar{f}_{1q} f_{1q}^{\perp q}}{M_2} \right] \\ &- \sin^2\theta \sin(\phi + \phi_{S_2}) \\ &\left. \times \mathcal{F}\left[\hat{\mathbf{h}} \cdot \mathbf{k}_{1T} \frac{\bar{h}_{1q}^\perp h_{1q}^\perp}{M_1} \right] \right\}. \quad (2) \end{aligned}$$

Here $\hat{\mathbf{h}} \equiv \mathbf{q}_T/|\mathbf{q}_T|$, $h_{1q}(x, \mathbf{k}_T^2)$ is the k_T -dependent transversity distribution, while $h_{1q}^\perp(x, \mathbf{k}_T^2)$ and $f_{1q}^\perp(x, \mathbf{k}_T^2)$ are k_T -dependent T-odd PDFs (see Ref. [1] for review). The convolution product is defined [2] as

$$\begin{aligned} \mathcal{F}[\bar{f}_q f_q] &\equiv \int d^2\mathbf{k}_{1T} d^2\mathbf{k}_{2T} \delta^2(\mathbf{k}_{1T} + \mathbf{k}_{2T} - \mathbf{q}_T) \\ &\times [f_q(x_1, \mathbf{k}_{1T}^2) \bar{f}_q(x_2, \mathbf{k}_{2T}^2) + (1 \leftrightarrow 2)]. \quad (3) \end{aligned}$$

Let us first consider the purely unpolarized DY process. Notice that Eq. (1) is very inconvenient in application because of the complicated q_T - and k_T -dependence enter-

^{*}Electronic address: sisakian@jinr.ru

[†]Electronic address: shev@mail.cern.ch

[‡]Electronic address: nagajcev@mail.desy.de

[§]Electronic address: ivon@jinr.ru

¹See [1] for details of the respective kinematics.

ing Eq. (1) via the convolution, Eq. (3). To deal with Eq. (1) the model

$$h_{1q}^\perp(x, \mathbf{k}_T^2) = \frac{\alpha_T}{\pi} c_H^q \frac{M_C M_H}{\mathbf{k}_T^2 + M_C^2} e^{-\alpha_T \mathbf{k}_T^2} f_{1q}(x), \quad (4)$$

where $M_C = 2.3$ GeV, $c_H^q = 1$, $\alpha_T = 1$ GeV⁻², and M_H is the hadron mass, was proposed in Ref. [2]. With such an assumption one then calculates [2,3] the coefficient $\kappa \equiv \nu/2$ at the $\cos 2\phi$ dependent part of the ratio

$$R \equiv \frac{d\sigma^{(0)}/d\Omega}{\sigma^{(0)}}, \quad (5)$$

which allows us to explain² the anomalous $\cos 2\phi$ -dependence [4,5] of the unpolarized DY cross-section. However, the author of Ref. [2] stresses that Eq. (4) is just a ‘‘crude model.’’ Besides, Eq. (4) cannot help us to extract the quantity h_1^\perp from the unpolarized DY process.

Thus, to avoid these problems, let us apply the \mathbf{q}_T weighting approach which was first proposed and applied in Refs. [6,7] with respect to a particular electron-positron annihilation process and in Ref. [8] with respect to semi-inclusive DIS. To use the advantage of the \mathbf{q}_T integration, one should extract from the unpolarized DY process the properly integrated over \mathbf{q}_T ratio [cf. Eq. (5)]

$$\hat{R} = \frac{\int d^2 \mathbf{q}_T [|\mathbf{q}_T|^2 / M_1 M_2] [d\sigma^{(0)}/d\Omega]}{\int d^2 \mathbf{q}_T \sigma^{(0)}}, \quad (6)$$

parametrized as

$$\hat{R} = \frac{3}{16\pi} (\gamma(1 + \cos^2\theta) + \hat{k} \cos 2\phi \sin^2\theta), \quad (7)$$

that should be compared³ with the equation (see Refs. [2,4])

$$R = \frac{3}{16\pi} (1 + \lambda \cos^2\theta + \mu \sin 2\theta \cos\phi + (\nu/2) \cos 2\phi \sin^2\theta) \quad (\nu \equiv 2\kappa, \lambda \simeq 1, \mu \simeq 0). \quad (8)$$

By virtue of Eq. (1), the coefficient \hat{k} at the $\cos 2\phi$ -dependent part of \hat{R} reads

$$\hat{k} = \int d^2 \mathbf{q}_T [|\mathbf{q}_T|^2 / M_1 M_2] \sum_q e_q^2 \mathcal{F} \left[(2\hat{\mathbf{h}} \cdot \mathbf{k}_{1T} \hat{\mathbf{h}} \cdot \mathbf{k}_{2T} - \mathbf{k}_{1T} \cdot \mathbf{k}_{2T}) \frac{\bar{h}_1^\perp h_1^\perp}{M_1 M_2} \right] \left(\int d^2 \mathbf{q}_T \sum_q e_q^2 \mathcal{F} [\bar{f}_1 f_1] \right)^{-1}, \quad (9)$$

²Notice that the large values of ν cannot be explained by leading and next-to-leading order perturbative QCD corrections as well as by the high twists effects (see [2] and references therein).

³Obtaining Eg. (8) one sets [2] $\lambda = 1$ and $\mu = 0$ in the most general equation for R (Eq. (5) in Ref. [2]), which is justified [2] by the expectation from next-to-leading order QCD and the data (Refs. [4,5]) in the Collins-Soper frame.

and, due to the properly chosen weight $|\mathbf{q}_T|^2$, the integration over \mathbf{q}_T leads to⁴ the following simple equation for \hat{k} :

$$\hat{k} = 8 \frac{\sum_q e_q^2 (\bar{h}_{1q}^{\perp(1)}(x_1) h_{1q}^{\perp(1)}(x_2) + (1 \leftrightarrow 2))}{\sum_q e_q^2 (\bar{f}_{1q}(x_1) f_{1q}(x_2) + (1 \leftrightarrow 2))}, \quad (10)$$

where the standard notation [6–8]

$$h_{1q}^{\perp(n)}(x) \equiv \int d^2 \mathbf{k}_T \left(\frac{\mathbf{k}_T^2}{2M^2} \right)^n h_{1q}^\perp(x, \mathbf{k}_T^2) \quad (11)$$

for the n th moment of the \mathbf{k}_T -dependent PDF is used. Thus, one can see that the numerator of \hat{k} is factorized out in the simple product of the first moments of h_1^\perp distributions. This allows us to directly extract these quantities from \hat{k} , which should be measured in unpolarized DY. This, in turn (see below), allows us to directly extract the transversity distributions h_1 from the single-spin polarized DY. Notice that now there is no need in any model assumptions about k_T -dependence of h_1^\perp distributions.

Let us now consider the single transversely polarized DY process $H_1 H_2^+ \rightarrow l^+ l^- X$ and define the following single-spin asymmetries (SSA)

$$A_{h(f)} = \int d\Omega d\phi_{S_2} \sin(\phi \pm \phi_{S_2}) [d\sigma(\mathbf{S}_{2T}) - d\sigma(-\mathbf{S}_{2T})] \times \left(\int d\Omega d\phi_{S_2} [d\sigma(\mathbf{S}_{2T}) + d\sigma(-\mathbf{S}_{2T})] \right)^{-1}, \quad (12)$$

where the single-polarized cross-section is given by Eq. (2). It is clear that in the difference $d\sigma(\mathbf{S}_{2T}) - d\sigma(-\mathbf{S}_{2T})$, only the terms of Eq. (12) containing $\sin(\phi - \phi_{S_2})$ and $\sin(\phi + \phi_{S_2})$ survive (and are multiplied by two). Besides, the properly chosen⁵ weights $\sin(\phi + \phi_{S_2})$ and $\sin(\phi - \phi_{S_2})$ allow us to separate the contributions containing the h_1^\perp and f_{1T}^\perp PDFs with the result

$$A_h = -\frac{1}{4} \frac{\sum_q e_q^2 \mathcal{F} \left[\frac{\hat{\mathbf{h}} \cdot \mathbf{k}_{1T}}{M_1} \bar{h}_{1q}^\perp h_{1q} \right]}{\sum_q e_q^2 \mathcal{F} [\bar{f}_{1q} f_{1q}]}, \quad (13)$$

and

$$A_f = \frac{1}{2} \frac{\sum_q e_q^2 \mathcal{F} \left[\frac{\hat{\mathbf{h}} \cdot \mathbf{k}_{2T}}{M_2} \bar{f}_{1q}^q f_{1T}^{\perp q} \right]}{\sum_q e_q^2 \mathcal{F} [\bar{f}_{1q} f_{1q}]}. \quad (14)$$

The asymmetries like A_f given by Eqs. (12) and (14) and their application with respect to Sivers function $f_{1T}^\perp(x, \mathbf{k}_T^2) \equiv -(M/2|\mathbf{k}_T|) \Delta_{q/H}^N(x, \mathbf{k}_T^2)$ extraction from

⁴The normalization condition $\int d^2 \mathbf{k}_T f_{1q}(x, \mathbf{k}_T^2) = f_{1q}(x)$ is used (see, for example, Ref. [1]).

⁵The analogous weighting procedure was applied [9] in the case of transversely polarized semi-inclusive DIS by the HERMES collaboration.

the data were considered in detail in Refs. [10,11], so that we concentrate here on the asymmetry A_h given by Eqs. (12) and (13).

Notice that asymmetry A_h given by Eqs. (12) and (13) is inconvenient in application because of the complicated q_T -

and k_T -dependence entering the convolution. So, we again apply the q_T integration method [6–8] (see also its application for the SIDIS processes in Ref. [9] and for the Sivers PDF extraction from the single-polarized DY in Ref. [10]):

$$\hat{A}_h = \frac{\int d\Omega d\phi_{S_2} \int d^2\mathbf{q}_T (|\mathbf{q}_T|/M_1) \sin(\phi + \phi_{S_2}) [d\sigma(\mathbf{S}_{2T}) - d\sigma(-\mathbf{S}_{2T})]}{\int d\Omega d\phi_{S_2} \int d^2\mathbf{q}_T [d\sigma(\mathbf{S}_{2T}) + d\sigma(-\mathbf{S}_{2T})]}, \quad (15)$$

so that one easily gets

$$\hat{A}_h = -\frac{1}{2} \frac{\sum_q e_q^2 [\bar{h}_{1q}^{\perp(1)}(x_1) h_{1q}(x_2) + (1 \leftrightarrow 2)]}{\sum_q e_q^2 [\bar{f}_{1q}(x_1) f_{1q}(x_2) + (1 \leftrightarrow 2)]}. \quad (16)$$

Thus, one can see that \hat{A}_h is also factorized in the simple product of $\bar{h}_1^{\perp(1)}$ and h_1 .

Among a variety of DY processes, DY processes with antiprotons ($\bar{p}p \rightarrow l^+l^-X$, $\bar{p}p^1 \rightarrow l^+l^-X$, $\bar{p}^1p^1 \rightarrow l^+l^-X$) have an essential advantage because the charge conjugation symmetry can be applied. Indeed, due to charge conjugation, antiquark PDFs from the antiprotons are equal to the respective quark PDFs from the protons. Thus, Eqs. (10) and (16) in the case of $\bar{p}p$ collisions are rewritten as

$$\hat{k}|_{\bar{p}p^1 \rightarrow l^+l^-X} = 8 \frac{\sum_q e_q^2 [h_{1q}^{\perp(1)}(x_1) h_{1q}^{\perp(1)}(x_2) + \bar{h}_{1q}^{\perp(1)}(x_1) \bar{h}_{1q}^{\perp(1)}(x_2)]}{\sum_q e_q^2 [f_{1q}(x_1) f_{1q}(x_2) + \bar{f}_{1q}(x_1) \bar{f}_{1q}(x_2)]}, \quad (17)$$

and

$$\hat{A}_h|_{\bar{p}p^1 \rightarrow l^+l^-X} = -\frac{1}{2} \frac{\sum_q e_q^2 [h_{1q}^{\perp(1)}(x_1) h_{1q}(x_2) + \bar{h}_{1q}(x_1) \bar{h}_{1q}^{\perp(1)}(x_2)]}{\sum_q e_q^2 [f_{1q}(x_1) f_{1q}(x_2) + \bar{f}_{1q}(x_1) \bar{f}_{1q}(x_2)]}, \quad (18)$$

where now all PDFs refer to protons. Neglecting squared antiquark and strange quark PDF contributions to proton and taking into account the quark charges and u quark dominance at large⁶ x , Eqs. (17) and (18) are essentially given by

$$\hat{k}(x_1, x_2)|_{\bar{p}p^1 \rightarrow l^+l^-X} \simeq 8 \frac{h_{1u}^{\perp(1)}(x_1) h_{1u}^{\perp(1)}(x_2)}{f_{1u}(x_1) f_{1u}(x_2)}, \quad (19)$$

and

$$\hat{A}_h(x_1, x_2)|_{\bar{p}p^1 \rightarrow l^+l^-X} \simeq -\frac{1}{2} \frac{h_{1u}^{\perp(1)}(x_1) h_{1u}(x_2)}{f_{1u}(x_1) f_{1u}(x_2)}. \quad (20)$$

One can see that the system of Eqs. (19) and (20) has a very simple and convenient form in application. Measuring the quantity \hat{k} in unpolarized DY [Eqs. (6) and (7)] and using Eq. (19), one can obtain the quantity $h_{1u}^{\perp(1)}$. Then, measuring SSA, Eq. (15), and using the obtained quantity $h_{1u}^{\perp(1)}$, one can eventually extract the transversity distribution h_{1u} using Eq. (20). Let us stress once again that now there is no need in any model assumptions about k_T -dependence of h_1^{\perp} distributions.

In order to obtain squares of $h_{1u}^{\perp(1)}$ and f_{1u} in Eqs. (19) and (20), one should consider them at the points⁷ $x_1 = x_2 \equiv x$ (i.e., $x_F \equiv x_1 - x_2 = 0$), so that

$$h_{1u}^{\perp(1)}(x) = f_{1u}(x) \sqrt{\frac{\hat{k}(x, x)}{8}}, \quad (21)$$

and

$$h_{1u}(x) = -4\sqrt{2} \frac{\hat{A}_h(x, x)}{\sqrt{\hat{k}(x, x)}} f_{1u}(x). \quad (22)$$

To estimate the possibility of $h_{1u}^{\perp(1)}$ and h_{1u} measurement, the special simulation of DY events with the PAX kinematics [12] are performed. The proton-antiproton collisions are simulated with the PYTHIA event generator [13]. Two samples are prepared: for the collider mode (15 GeV antiproton beam colliding on the 3.5 GeV proton beam) and for the fixed target mode (22 GeV antiproton beam colliding on an internal hydrogen target). Each sample contains about 100 K pure Drell-Yan events. Notice, that this is just the statistics planned to be achieved by PAX. Indeed (see Ref. [12]), the sample for collider mode cor-

⁶The large x values is the peculiarity of the $\bar{p}p$ experiments planned at GSI—see Ref. [12]

⁷The different points $x_F = 0$ can be reached changing Q^2 value at fixed $s = x_1 x_2 Q^2 \equiv \tau Q^2$.

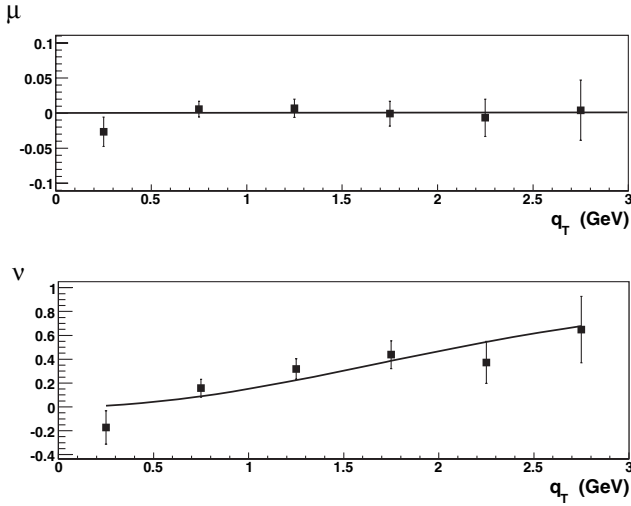


FIG. 1. Reconstructed from simulations (fixed target mode) quantities μ and ν versus q_T in comparison with the input (corresponding to experimental data) dependencies (solid lines).

responds to about 1 yr of data-taking with a cross-section of 40 mb and a luminosity of $2 \times 10^{30} \text{ cm}^{-2}\text{s}^{-1}$. For the fixed target mode it can take about three months with a cross-section of 30 mb and a luminosity of about $10^{31} \text{ cm}^{-2}\text{s}^{-1}$.

Unfortunately, the original PYTHIA generator we deal with does not reproduce the corresponding to DY experiments [4,5] nontrivial q_T and x dependencies of the quantity ν entering Eq. (8). So, to estimate the possibility of $h_{1u}^{\perp(1)}$ and h_{1u} measurement, one should properly introduce these dependencies in accordance with the existing experimental data. To this end we apply the commonly used Monte Carlo method based on weighting of the kinematical events. To apply the weighting procedure in our case, we just ascribe to each event the weight $w = R$ which, in accordance with the data [4,5], is given by Eq. (8), where $\lambda \simeq 1$, $\mu \simeq 0$, and ν has nontrivial q_T and x dependencies. The q_T dependence of ν is taken from Refs. [2,3]—Eq. (49) in Ref. [2] and Eq. (21) in Ref. [3], and this q_T dependence properly fits the existing experimental data [4,5]. However, in Refs. [2,3] (where the simplified Boer's model is applied) there is no (important and corresponding to DY experiments [4,5]) x -dependence of ν at all, so that we take this dependence from Ref. [4].

To check the validity of the angular distribution analysis of the weighted events we reconstruct the q_T and x_1 dependencies of ν . The results are shown in Figs. 1 and 2. One can see a good agreement⁸ between input (solid lines) and reconstructed (points with error bars) values.

Thus, applying the above-described weighting procedure, our simulations reproduce the nontrivial angular dependence of R with q_T - and x -dependent ν . These de-

⁸As an additional check of our analysis validity, we reproduce the input zero value of μ .

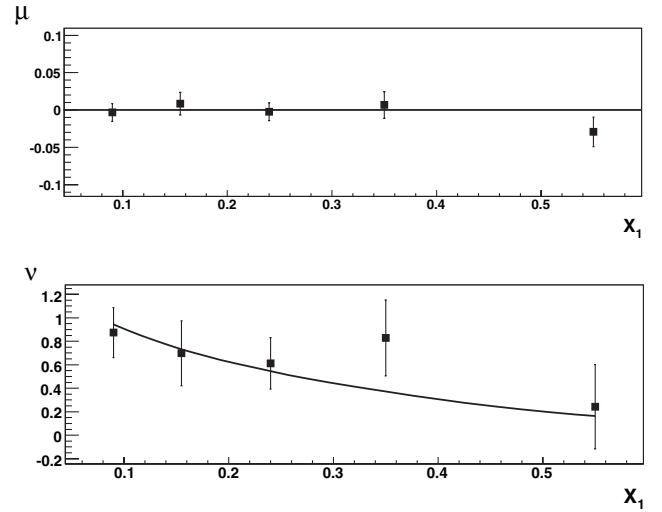


FIG. 2. Reconstructed from simulations (fixed target mode) quantities μ and ν versus x_1 in comparison with the input (corresponding to experimental data) dependencies (solid lines).

pendencies are in accordance with the respective input dependencies obtained in experiments on DY [4,5]. Now it is straightforward to reconstruct the q_T -weighted quantity \hat{R} [Eq. (6)] and, consequently, \hat{k} [Eq. (7)]. The results are shown in Fig. 3. The values of \hat{k} at averaged Q^2 for both modes are found to be 1.2 ± 0.2 for the collider mode and 1.0 ± 0.2 for the fixed target mode.

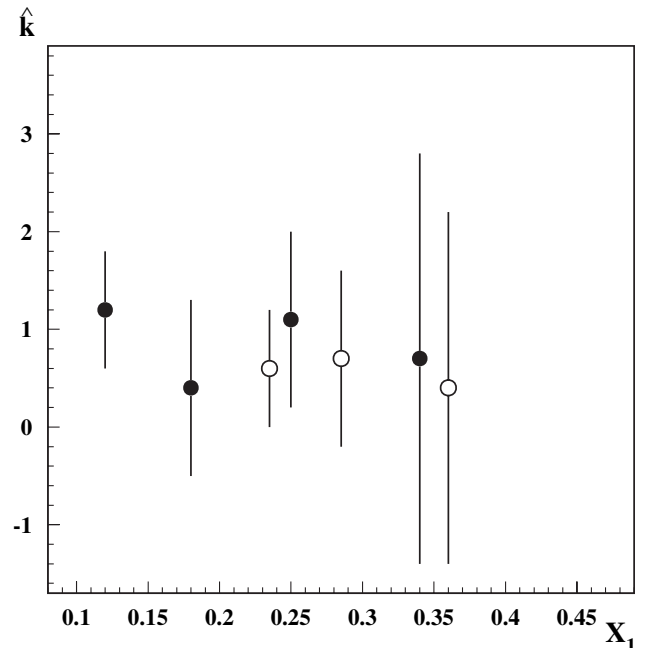


FIG. 3. \hat{k} versus x_1 at $x_F \simeq 0$. Data is obtained with Monte Carlo simulations for the collider mode (closed circles) and for the fixed target mode (open circles). For better visibility (to avoid overlapping), the points for the collider (fixed target) mode are shifted 0.01 to the left (right) along the x -axis.

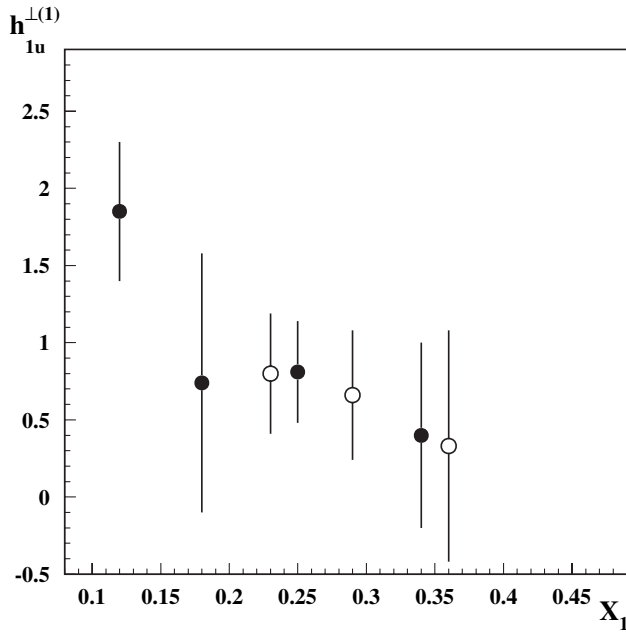


FIG. 4. $h_{1u}^{\perp(1)}$ versus x_1 at $x_F \approx 0$. Data is obtained with Monte Carlo simulations for the collider mode (closed circles) and for the fixed target mode (open circles). For better visibility (to avoid overlapping), the points for the collider (fixed target) mode are shifted 0.01 to the left (right) along the x -axis.

The quantity $h_{1u}^{\perp(1)}$ is reconstructed from the obtained values of \hat{k} using Eq. (21) with $x_F = 0 \pm 0.04$. The results are shown in Fig. 4. The obtained magnitudes of $h_{1u}^{\perp(1)}$ are in accordance (in order of value) with the respective magnitudes obtained with the model (4) for $h_{1u}^{\perp}(x, \mathbf{k}_T)$. Indeed, for example, for the collider mode ($Q_{\text{average}}^2 \approx 9 \text{ GeV}^2$, so that $x_1 \approx x_2 \approx 0.2$ at the point $x_F \approx 0$), the results from the simulations and from the model (4) are $h_{1u}^{\perp(1)} \approx 1$ and $h_{1u}^{\perp(1)} \approx 0.5$, respectively.

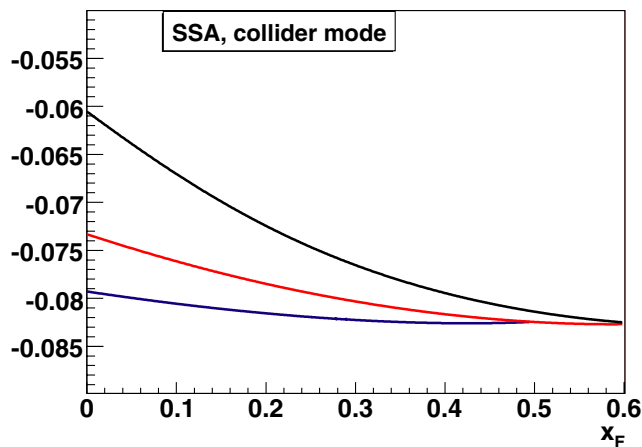


FIG. 5 (color online). SSA given by Eq. (20) versus x_F for the collider mode for three values of Q^2 : 50 GeV^2 (lower curve), 25 GeV^2 (middle curve), and 9 GeV^2 (upper curve).



FIG. 6 (color online). SSA given by Eq. (20) versus x_F for the fixed target mode for three values of Q^2 : 16 GeV^2 (lower curve), 9 GeV^2 (middle curve), and 4 GeV^2 (upper curve).

Using the obtained magnitudes of $h_{1u}^{\perp(1)}$ we estimate the expected SSA given by Eq. (20). The results are shown in Figs. 5 and 6. For estimation of h_{1u} entering SSA together with $h_{1u}^{\perp(1)}$ [see Eq. (20)], we follow the procedure of Ref. [14] and use the (rather crude) “evolution model” [2,14], where there are no estimations of uncertainties. That is why in (purely qualitative) Figs. 5 and 6 we present the solid curves instead of points with error bars. To obtain these curves we reproduce the x -dependence of $h_{1u}^{\perp(1)}$ in the considered region, using the Boer’s model, Eq. (4), properly numerically corrected in accordance with the simulation results.

To estimate the measurability of the quantities we deal with, it is relevant to estimate the upper bounds on h_1 , $h_1^{\perp(1)}$ and then on \hat{k} and \hat{A}_h . Obtaining $h_{1u}^{\perp(1)}$ and h_{1u} one deals with Eqs. (19) and (20) applied at the points $x_1 \approx x_2 \approx \sqrt{Q^2}/s$, so that we perform the estimation of the upper bounds on \hat{k} and \hat{A}_h at the points $x_F \approx 0$ corresponding to the average Q^2 values for both the collider and fixed target modes. The maximally allowed value of $h_1^{\perp(1)}$ can be found operating just as it was done with respect to the quantity $f_{1T}^{\perp(1)q}$ (first moment of the Sivers function) in Ref. [10]. To this end we first apply the inequality [15]⁹ ($|\mathbf{k}_T|/M)h_1^{\perp}(x, \mathbf{k}_T^2) \leq f_1(x, \mathbf{k}_T^2)$). Then, using the estimation (see Ref. [10] and references therein) $\langle k_T \rangle \approx 0.8 \text{ GeV}$, one easily gets the upper bound on $h_{1u}^{\perp(1)}$: $h_{1u}^{\perp(1)} \leq 0.4f_{1u}(x)$. On the other hand, the maximally allowed value of h_{1u} can be found using the Soffer [16] inequality $|h_{1u}| \leq (f_{1u} + g_{1u})/2$. For the PAX kinematics $s = 43 \text{ GeV}^2$, $Q_{\text{average}}^2 \approx 5 \text{ GeV}^2$ for the fixed target mode

⁹This inequality is directly obtained by relaxing the bound Eq. (16) in Ref. [15] (eliminating the unknown distribution in that bound).

and $s = 215 \text{ GeV}^2$, $Q_{\text{average}}^2 \simeq 9 \text{ GeV}^2$ for the collider mode. Thus, at the point $x_F = 0$ we deal with, $x_1 \simeq x_2 \simeq 0.3$ and $x_1 \simeq x_2 \simeq 0.2$ for the fixed target and collider modes, respectively. Then, the inequalities on h_{1u} and $h_{1u}^{\perp(1)}$ give¹⁰ $h_{1u(\text{max})} \simeq 1.5$ ($f_{1u} = 1.9$, $g_{1u} = 1.0$) and $h_{1u(\text{max})}^{\perp(1)} \simeq 0.8$ for the fixed target mode while $h_{1u(\text{max})} \simeq 2.3$ ($f_{1u} = 3.1$, $g_{1u} = 1.5$) and $h_{1u(\text{max})}^{\perp(1)} \simeq 1.2$ for the collider mode. Using these estimations of $h_{1u(\text{max})}$ and $h_{1u(\text{max})}^{\perp(1)}$ in Eqs. (19) and (20), it is straightforward to obtain the maximally allowed values of \hat{k} and \hat{A}_h : $\hat{k}_{(\text{max})} \simeq 1.4$ and $|\hat{A}_{h(\text{max})}| \simeq 0.17$ for the fixed target mode while $\hat{k}_{(\text{max})} \simeq 1.2$ and $|\hat{A}_{h(\text{max})}| \simeq 0.14$ for the collider mode. One can see that obtained estimations of upper bounds on $h_{1u}^{\perp(1)}$, \hat{k} and \hat{A}_h are in accordance with the results presented by Figs. 3–6.

Looking at the (preliminary) estimations presented by Figs. 3 and 4, one can conclude that the quantities \hat{k} and $h_{1u}^{\perp(1)}$ are presumably measurable in most of the considered x -region. At the same time, looking at Figs. 5 and 6 one can see that for both modes SSA, \hat{A}_h is estimated to be about 6%–8%. On the other hand, as it was argued in Ref. [12] (see section “Single Spin Asymmetries and Sivers Function”, p. 25), the SSA studied in Ref. [10], $A_{UT}^{\sin(\phi - \phi_S)(q_T/M_N)}$, of order 5%–10% can be measured by PAX. It is obvious that the SSA studied in this paper, \hat{A}_h , weighted with $\sin(\phi + \phi_S)$ and the same weight q_T/M_N , is absolutely analogous to SSA $A_{UT}^{\sin(\phi - \phi_S)(q_T/M_N)}$, so that it is clear that if $A_{UT}^{\sin(\phi - \phi_S)(q_T/M_N)}$

¹⁰Performing these estimations we use GRSV2000LO parametrization [17] for g_{1u} and GRV98LO parametrization [18] for f_{1u} .

of 5%–10% is measurable, then \hat{A}_h of 6%–8% is measurable too.

Thus, it is shown that it is possible to directly extract the transversity and its accompanying T-odd PDF from the unpolarized and single-polarized DY processes with anti-proton participation. It is of importance that there is no need in any model assumptions about k_T -dependence of h_1^\perp . One can directly extract both h_1 and the first moment of h_1^\perp from the single-polarized and unpolarized DY processes, since these quantities enter the measured \hat{k} and SSA A_h in the form of simple product instead of complex convolution. The preliminary estimations for PAX kinematics show the possibility to measure both \hat{k} and SSA \hat{A}_h and then to extract the quantities $h_1^{\perp(1)}$ and h_1 . Certainly, the estimations of \hat{k} and \hat{A}_h magnitudes obtained in this paper are very preliminary and show just the order of values of these quantities. For more precise estimations one needs the Monte Carlo generator, which is more suitable for DY processes studies (see, for example, Ref. [3]) than the PYTHIA generator which we used (with the proper weighting of events) here.

Notice that it is straightforward to properly modify the procedure discussed in this paper to DY processes: $\pi^- p \rightarrow \mu^+ \mu^- X$ and $\pi^- p^\dagger \rightarrow \mu^+ \mu^- X$, which could be studied [19] in the COMPASS experiment at CERN.

The authors are grateful to M. Anselmino, R. Bertini, O. Denisov, A. Efremov, A. Kacharava, V. Krivokhizhin, A. Kulikov, P. Lenisa, A. Maggiora, A. Olshevsky, G. Piragino, G. Pontecorvo, F. Rathmann, I. Savin, M. Tabidze, O. Teryaev and W. Vogelsang for fruitful discussions. The work of O. S. and O. I. was supported by the Russian Foundation for Basic Research (Project No. 05-02-17748).

-
- [1] V. Barone, A. Drago, and P. G. Ratcliffe, *Phys. Rep.* **359**, 1 (2002).
 - [2] D. Boer, *Phys. Rev. D* **60**, 014012 (1999).
 - [3] A. Bianconi and M. Radici *Phys. Rev. D* **71**, 074014 (2005).
 - [4] J. S. Conway *et al.*, *Phys. Rev. D* **39**, 92 (1989).
 - [5] S. Falciano *et al.* (NA10 Collaboration), *Z. Phys. C* **31**, 513 (1986); M. Guanziroli *et al.* (NA10 Collaboration), *Z. Phys. C* **37**, 545 (1988).
 - [6] D. Boer, R. Jakob, and P. J. Mulders, *Nucl. Phys.* **B504**, 345 (1997).
 - [7] D. Boer, R. Jakob, and P. J. Mulders, *Phys. Lett. B* **424**, 143 (1998).
 - [8] D. Boer and P. J. Mulders, *Phys. Rev. D* **57**, 5780 (1998).
 - [9] A. Airapetian *et al.* (HERMES Collaboration), *Phys. Rev. Lett.* **84**, 4047 (2000); *Phys. Rev. D* **64**, 097101 (2001); *Phys. Lett. B* **562**, 182 (2003); *Phys. Rev. Lett.* **94**, 012002 (2005).
 - [10] A. V. Efremov *et al.*, *Phys. Lett. B* **612**, 233 (2005).
 - [11] M. Anselmino, U. D’Alesio, and F. Murgia, *Phys. Rev. D* **67**, 074010 (2003).
 - [12] V. Barone *et al.* (PAX Collaboration), Antiproton-Proton Scattering Experiments with Polarization, Julich, April 2005, http://www.fz-juelich.de/ikp/pax/public_files/tp_PAX.pdf
 - [13] T. Sjostrand *et al.*, hep-ph/0308153.
 - [14] M. Anselmino, V. Barone, A. Drago, and N. N. Nikolaev, *Phys. Lett. B* **594**, 97 (2004).
 - [15] A. Bacchetta, M. Boglione, A. Henneman, and P. J. Mulders, *Phys. Rev. Lett.* **85**, 712 (2000).
 - [16] J. Soffer, *Phys. Rev. Lett.* **74**, 1292 (1995).
 - [17] M. Gluck, E. Reya, M. Stratmann, and W. Vogelsang, *Phys. Rev. D* **63**, 094005 (2001).
 - [18] M. Gluck, E. Reya, and A. Vogt, *Eur. Phys. J. C* **5**, 461 (1998).
 - [19] R. Bertini *et al.* (private communication).